Novel thermoelectric Bi_2Te_3 nanotubes and nanocapsules prepared by hydrothermal synthesis

X.H. Ji[1, 2], X.B. Zhao[1], Y.H. Zhang[1], T.Sun[1], H.L. Ni[1] B.H. Lu[1]
[1] State Key Laboratory of Silicon Materials, Zhejiang University, 310027 Hangzhou, China
[2] Institute of Materials Science and Engineering, Taiyuan University of Technology, 030024 Taiyuan, China
Email: zhaoxb@zju.edu.cn, Tel: +86-571-87951451, Fax: +86-571-87911171

Abstract

Bi_2Te_3 nano-powders have been prepared via hydrothermal synthesis in closed and opened systems respectively by using Te powder and $BiCl_3$ as the reactants and $NaBH_4$ as the reductant. The morphology and microstructure investigations of the products show that novel quasi-one-dimensional Bi_2Te_3 nanotubes and nanocapsules with an average diameter of about 100nm have formed during the reactions. The nanotubes-contained powder was used as the additive of hot-pressed Bi_2Te_3 based alloys. Thermoelectric transport measurements show that the thermoelectric properties of the nano-composite bulk materials are remarkably increased. The maximum figure of merit *ZT* above 1.2 was achieved.

1. Introduction

One-dimensional (1D) materials such as various kinds of nanowires and nanotubes have attracted considerable attention recently, because of their potential applications in nano-electronic and energy conversion devices [1-3]. Dresselhaus *et al* predicted that the use of low-dimensional systems would increase the figure of merit of thermoelectric (TE) materials significantly [4].

Bismuth telluride, Bi_2Te_3, and its alloys are the most important TE materials used in state-of-the-art devices for the 200 - 400K temperature range. Many works have been done in recent years to improve their figure of merit by making the material nanostructured including nanowire arrays [5,6] and quantum dot superlattice thin films [7,8]. The highest figure of merit even observed was reported by Venkatasubramanian and co-workers with $ZT = 2.4$ at room temperature for the p-type Bi_2Te_3/Sb_2Te_3 superlattice thin film [7]. Bi_2Te_3 nanowires or nanorods have been prepared by electrochemical deposition [9]. Low temperature routes, such as solvothermal or hydrothermal synthesis, have been used recently to prepare nanostructured Bi_2Te_3 based alloys [10-14]. These chemical routes have the advantages of low synthesis temperatures and fine grain sizes in comparison with those by a high temperature route such as melting process. Many morphologies of solvothermally or hydrothermally synthesized Bi_2Te_3 powders have been reported [11,12,14], including nanorods, polygonal nanosheets, polyhedral nanoparticles and sheet-rods.

Novel fullerene-related structures like nanotubes would be very interesting to improve the TE properties of bismuth telluride based materials, since nanotubes possess both holey structure [15] and low-dimensional features, and could be a phonon-glass/electron-crystal (PGEC) [16]. Bi_2Te_3 has a quasi-layered lattice structure. In each five atomic layers along the *c*-axis of Bi_2Te_3 there is a van-der-Waal bonding between two Te-layers. This makes it possible for Bi_2Te_3 to form a nanotube. But to the best of our knowledge, no Bi_2Te_3 nanotubes have been prepared till now. In this work, we report the hydrothermal syntheses of nanostructured Bi_2Te_3 containing a large portion of nanotubes or nanocapsules, and the promising application of the nanostructured powder on the improvement of the TE properties of Bi_2Te_3 based bulk nano-composite material has been investigated.

2. Experimental

All chemicals used for the synthesis of nanostructured Bi_2Te_3 in the present work are analytical grade without further purification. Two synthesis routes were used in the present work. Route-A is a high temperature (>120°C) synthesis route in a closed reaction system using a 500 mL teflon-lined autoclave. Route-B uses a temperature below the boiling point of water and processes in an 800 mL glass beaker. In a typical synthesis process, 30 mmol tellurium powder (5N purity, ≤ 30 μm), 20 mmol $BiCl_3$ and 2g ethylene-diamine-tetra-acetic disodium salt (EDTA) were mixed with 400 mL distilled water in the autoclave for Route-A or the glass beaker for Route-B. Then 3.5 g NaOH as pH-controller and 3.5 g $NaBH_4$ as reductant were added in the solution. The autoclave was sealed immediately after the charge of reductant. The system was heated to the reaction temperature of 150°C for Route-A or 65°C for Route-B, respectively, with a heating rate of about 5°C/min. During the reaction, the solution was stirred by a stainless steel stirrer with a rotational speed of about 60 rpm. After a reaction time at the designed temperature of 24h for Route-A or 37h for Route-B, the system was cooled naturally down to room temperature. The dark grey powders in the autoclave or the glass beaker were filtered, washed with distilled water and ethanol several times, and then dried in vacuum at 100°C for 6 h.

The phase structures of the powders were investigated by X-ray diffraction (XRD) with a Rigaku D/MAX-2550P X-ray diffracter using Cu K_α radiation ($\lambda = 1.5406$Å), 2θ-step of 0.02° from 10° to 70°. Powder morphology was observed on a JEM-2010 transmission electron microscopy (TEM) and a Philips-CM20 high-resolution TEM (HRTEM).

The Seebeck coefficient α and electric conductivity σ were measured on a computer-assistant device. A temperature difference of about 4°C between cool and hot ends of the sample was used for the Seebeck coefficient measurements. Four-point-probe method was adopted for the electric conductivity measurement. The thermal conductivity κ was calculated by using $\kappa = a \rho C_P$, where ρ is the sample density estimated by an ordinary dimension and weight measurement, a and C_P, the thermal diffusivity and specific heat of the sample, were measured on a Netzsch LFA-427 and a DSC-404, respectively.

3. Results and discussion

The XRD patterns, Figure 1(a), indicate that the hydrothermally synthesized powders have a single rhombohedral phase of Bi_2Te_3 (space group of $R\bar{3}m$). The diffraction peaks of Bi_2Te_3 in Figure 1(a) can be exactly indexed with the standard diffraction planes of rhombohedral Bi_2Te_3 according to JCPDS 82-0358. The diffraction peaks of the powder synthesized by Route-B at 65°C are significantly broader than those corresponding to the sample by Route-A at 150°C, indicating that the crystal sizes are significantly dependent on the synthesis temperature. From the HRTEM image of the synthesized Bi_2Te_3 powder in Figure 1(b) we measured the distances between two neighbouring (110) planes and two (003) planes of 2.11Å and 10.03Å, respectively. The lattice parameters calculated from these measurements are a = 4.22Å and c = 30.09Å, which are a little smaller than the standard data given by JCPDS 82-0358, a = 4.395Å and c = 30.44Å, but are in the range of experimental errors.

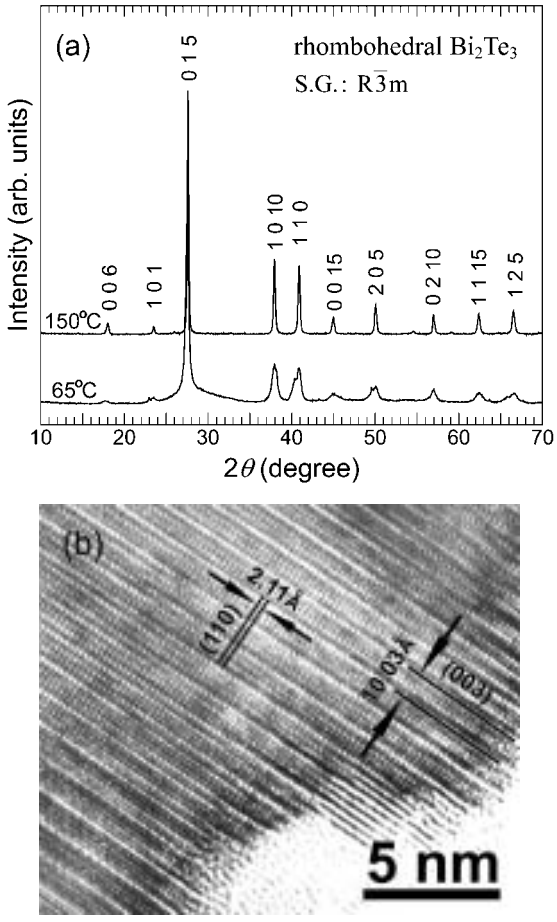

Figure 1: The XRD patterns (a) of the hydrothermally synthesized Bi_2Te_3 powders with the indexes of the diffraction planes of the $R\bar{3}m$ phase, and the HRTEM image (b) taking from the $<1\bar{1}0>$ direction showing the atomic structure of the Bi_2Te_3 powder.

Figure 2 gives the TEM and HRTEM photos taken from the powders hydrothermally synthesized with Route-A at 150°C in a sealed autoclave. Figure 2(a) shows a cluster of long nanotubes, along with some small nanoparticles. The nanotubes have the sizes of 30–100 nm in diameters and up to 1 μm or longer in lengths. Figure 2(b) shows three parallelly arranged nanotubes with closed ends. The electron diffraction pattern (EDP) inserted in the figure indicates that the tubes are of single crystalline. From the HRTEM image of a Bi_2Te_3 nanotube, Figure 2(c), we obtain the thickness of the tube-wall being about 20nm, which means it is a multi-wall nanotube. Figure 2(c) shows also that the tube wall is not smooth and neat but uneven and spiral. The enlarged photo of a small nanotube, Figure 2(d), reveals a typical structure of a tube wall. One sees that the c-axis of the Bi_2Te_3 rhombohedral lattice is at an angle of about 20° with the wall normal direction. The tilted atomic planes form a spiral wall like a continuously developed pencil-shaving as we can see also in Figure 2(c).

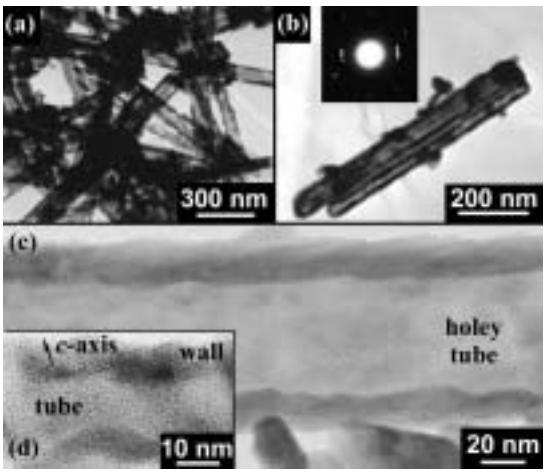

Figure 2: TEM and HRTEM images of the Bi_2Te_3 nanotubes hydrothermally synthesized in a closed system at 150°C.

The morphology of the nanopowder synthesized with Route-B in an opened system at 65°C is shown in Figure 3. To our interests, the powders have a novel morphology of bubble-like short nanotubes, which we called "nanocapsules". The sizes of the nanocapsules measured from Figure 3 are about 100 – 200nm in diameters and 300 – 1500nm in lengths. The wall thickness estimated from Figure 3(b) is less than 10nm, which corresponds to 2 or 3 times the lattice parameter in the c-axis of Bi_2Te_3, c = 3.044nm according to JCPDS 82-0358. The nanocapsule walls are significantly thinner than the nanotube walls formed by Route-A, Figure 2. This is also agree with the phenomena implied by the XRD pattern in Figure 1(a), that the crystal sizes of the powder synthesized with Route-B should be remarkable smaller those of the powder obtained by Route-A. The TEM image shows also that the most capsules have closed ends, as indicated by arrow A in Figure 3. Open ends, however, can also be found such as those denoted with arrow B in Figure 3. We also find that the capsules are often forked so they have several branches, arrow C in Figure 3. In the enlarged TEM photo of a branched nanocapsule, Figure 3(b), we see the angle between two branches is about 120°, corresponding to the hexagonal lattice structure of Bi_2Te_3. There are also small Bi_2Te_3 sheets (arrow D and E) in the powder. The thin sheets are curved as to be a nanocapsule segment (arrow E), which could be a fragment falling from a broken nanocapsule but might also be an unclosed developing capsule or a tube nucleus.

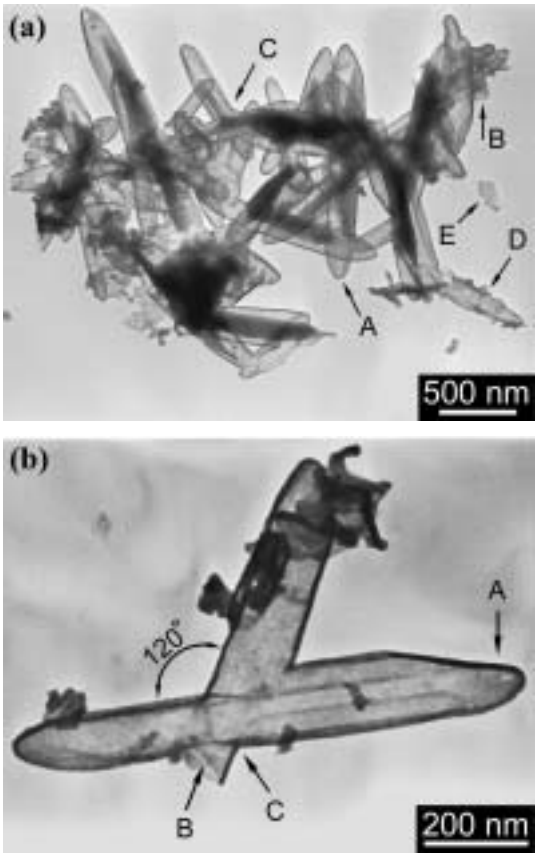

Figure 3: TEM images of the Bi_2Te_3 nanocapsules hydrothermally synthesized in an opened system at 65°C, showing closed ends (A), open ends (B), tube branching (C) and sheet segments (D and E).

We note that nanotubes are the combinative of both holey and low-dimensional materials. The basic Bi_2Te_3 crystal structure of the tube wall ensures an appropriate mobility for carriers, which makes the electrical conductivity of the material be high. The hollow tube channels and the low dimensional feature have a strong phonon scattering effect, which reduce the lattice thermal conductivity efficiently. The high electrical conductivity and low thermal conductivity make Bi_2Te_3 nanotubes be an attractive PGEC-like TE material. As a primary application, we used the Bi_2Te_3 nanotubes containing powder prepared with Route-A in the sealed system at 150°C as an additive of n-type Bi_2Te_3 TE materials. A zone-melted commercial n-type Bi_2Te_3 ingot was broken and milled to about 100μm in size, and then mixed with 15 weight percent of the uninstructed powder. The mixed powder was hot pressed in vacuum at 350°C for 30min using a pressure of 50MPa in a graphite die with a diameter of 16mm to form a nano-composite bulk TE material. The transport properties of the nano-composite samples were measured and plotted in Figure 4 in comparison with the data measured for the zone-melted sample. Considering the strong anisotropy of the zone-melted (directional solidified) Bi_2Te_3, the zone-melted sample for the transport property measurements was so cut from the ingot that the measuring direction would be the optimal crystal direction, i.e., parallel to the solidification direction of the ingot.

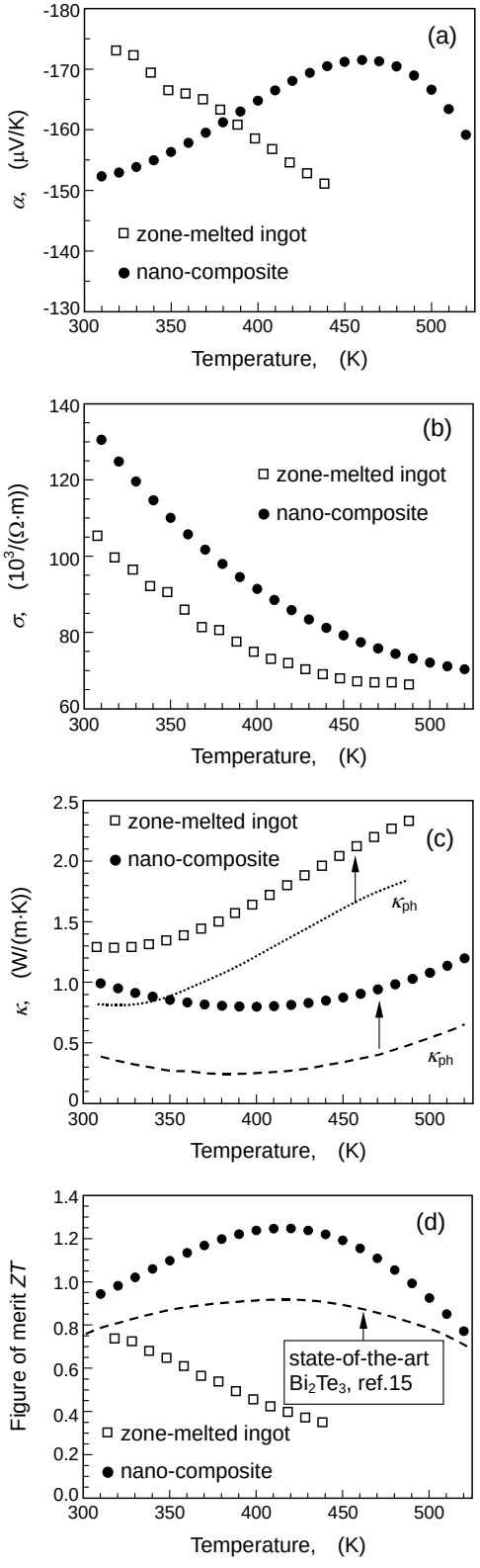

Figure 4: Transport properties of the nano-composite sample in comparison with the data measured from the zone-melted sample, for Seebeck coefficient (a), electrical conductivity (b), thermal conductivity (c) and dimensionless figure of merit (d). The lattice thermal conductivities are also plotted in (c) for the zone-melted sample (dotted line) and the nano-composite (dashed line).

Figure 4 showed the transport properties of the nano-composite sample in comparison with the data measured from the zone-melted sample. Both samples have the similar highest Seebeck coefficients between 170 and 175 μV/K, which, however, appeared at very different temperatures, Figure 4(a). The temperature corresponding to the highest Seebeck coefficient is near the room temperature for the zone-melted sample, but above 450K for the nano-composite sample. This means that the carrier transport mechanism for the nano-composite should be different from that applied in commercial zone-melted materials. A possible interpretation could be that the energy gap becomes wider and the temperature of instinct excitation increases when the material is nanostructured. We noted that the nano-composite sample has a significantly higher electrical conductivity, Figure 4(b), and a much lower thermal conductivity than the zone-melted sample, Figure 4(c), in the same time. The low thermal conductivity of the nano-composite sample originated clearly from its low phonon thermal conductivity. The total thermal conductivity κ consists of the phonon contribution (lattice part), κ_{ph}, and the carrier contribution (electronic part), κ_e. The later is related to the electrical conductivity σ with $\kappa_e = L_0 \sigma T$, where L_0 is the Lorenz number and approximately equal to 1.5×10^{-8} V^2/K^2 in a non-degenerate semiconductor [7]. Subtracting κ_e from the total κ, we plotted the remaining phonon contributions, κ_{ph}, in Figure 4(c) with a dashed for the nano-composite and a dotted line for the zone-melted sample. One sees that the phonon thermal conductivity of the nano-composite sample is only about 0.3 W/(m·K) in the temperature range below 200°C, which is only about one fourth of that of the zone-melted sample. This means that the lattice thermal conductivity has been efficiently minimized by nano-powder. The mechanism here suggested is the special transport behaviours of the nanotubes, i.e., the enhanced phonon scattering and heat blocking effect by the holey tubes and the high electron mobility along the tube walls. The dimensionless figure of merit, *ZT*, keeps well above 1.0 for the nano-composite sample in a large temperature range, which is not only remarkable higher than the zone-melted sample, but also higher than commercial state-of-the-art Bi_2Te_3 based materials [15]. The highest figure of merit reaches 1.25, which is also one of the highest values even reported for bulk Bi_2Te_3 based materials. It is significant since a small addition (15%) of nano-powder leads to a remarkable increase on the figure of merit of the material. A higher figure of merit could be expected by the doping optimization of both the nano-powder and the composite.

4. Conclusions

Novel Bi_2Te_3 nanotubes with uneven and spiral multi-walls and nanocapsules with thinner neat walls have been prepared by hydrothermal synthesis in closed and opened systems and at 150°C and 65°C, respectively. The low-dimensional morphology of nanotubes with holey-structure enables Bi_2Te_3 nanostructured powders to be a potential TE material with a high figure of merit. The primary experiment shows that a 15% additive of the nanostructured powder leads to a remarkable increase on the figure of merit of the Bi_2Te_3 based bulk TE material.

Acknowledgements

This work was supported by the National Natural Science Foundation of China, Grant N50171064, and the "863" Program of China, contract number 2002AA302406. The authors thank Prof. X. B. Zhang Dept. Materials Science and Engineering, Zhejiang University, for his great help.

References

1. Collins, P.G. *et al*, "Nanoscale Electronic Devices on Carbon Nanotubes," *Nanotechnology*, Vol. 9 (1998), pp. 153-157.
2. Cui, Y. *et al*, "Functional Nanoscale Electronic Devices Assembled Using Silicon Nanowire Building Blocks," *Science*, Vol. 291 (2001), pp. 851-853.
3. Dresselhaus, M.S. *et al*, "Quantum Wells and Quantum Wires for Potential Thermoelectric Applications," *Semiconduct. Semimet.*, Vol. 71 (2001), pp. 1-121.
4. Dresselhaus, M. S. *et al*, "Low-dimensional thermoelectric materials," *Phys. Solid State*, Vol. 41, No. 5 (1999), pp.679-682.
5. Sander, M. S. *et al*, "Fabrication of high-density, high aspect ratio, large-area bismuth telluride nanowire arrays by electrodeposition into porous anode alumina templates," *Adv. Mater*., Vol. 14, No. 9 (2002), pp. 665-667.
6. Martín-González, M. *et al*, "High-density 40 nm diameter Sb-rich $Bi_{2-x}Sb_xTe_3$ nanowire arrays," *Adv. Mater*., Vol. 15, No.12 (2003), pp.1003-1006.
7. Venkatasubramanian, R. E. *et al*, "Thin-film thermoelectric devices with high room-temperature figures of merit," *Nature*, Vol. 413 (2001), pp.597-602.
8. Harman, T. C *et al*, "Quantum dot superlattice thermoelectric materials and devices," *Science*, Vol. 297 (2002), pp. 2229-2232.
9. Prieto, A. L. *et al*, "Electrodeposition of Ordered Bi_2Te_3 Nanowires: Arrays," *J. Am. Chem. Soc.*, Vol. 123 (2001), pp. 7160-7161.
10. Yu, S. H. *et al*, "A new low temperature one-step route to metal chalcogenide semiconductors: PbE, Bi_2E_3 (E=S, Se, Te)," *J. Mater. Chem*., Vol. 8,No.9 (1998), pp.1949-1951.
11. Deng, Y. *et al*. "Solvothermal preparation and characterization of nanocrystalline Bi_2Te_3 powder with different morphology," *J. Phys. Chem. Solids*,Vol. 63 (2002), pp. 2119-2121.
12. Deng, Y. *et al*."Ligand-assisted control growth of chainlike nanocrystals," *Chem. Phys. Lett*. Vol.368 (2003),pp. 639-643.
13. Zhao, X. B. *et al*. "Solvothermal synthesis of nano-sized $La_xBi_{(2-x)}Te_3$ thermoelectric powders," *Inorg. Chem. Comm.* Vol.7 (2004), pp.386-388.
14. Zhao, X. B. *et al*. "Effect of solvent on the microstructures of nanostructured Bi_2Te_3 prepared by solvothermal synthesis," *J.Alloys Comp.* Vol.368 (2004), pp.349-352.
15. Tritt, T. M. "Thermoelectric materials: holey and unholey semiconductors," *Science* Vol. 283 (1999), pp.804-805.
16. Slack, G. A. *et al.* "Some properties of semiconducting $IrSb_3$", *J. Appl. Phys*. Vol.76 (1994), pp.1665-1671.